Central Park & Urban Heat Island Effect in New York City

Sophia Ladyzhets & Sally Green

***Abstract*— The urban heat island effect causes New York City to be significantly warmer compared to surrounding rural and suburban areas. Within NYC, however, temperatures vary noticeably between areas with more vegetation, such as Central Park, and areas densely packed with buildings. This report formulates a heat transfer model to predict maximum daily ground temperatures in vegetated and concrete areas within NYC. The model is derived based on governing conservation of energy equations and implemented on real data collected at weather stations over seven months from March through September, 2022. The modes of heat transfer considered for all ground types are solar radiation to the ground, convective heat transfer, and radiation to the sky. For vegetated ground, evaporative cooling is also included in the model. Predicted ground temperatures from the model reproduce expected trends from historical 2002 weather data, with average percent error in the 10-20% range. The model correctly calculates Central Park to have a lower temperature than surrounding areas in the summer, as supported by both historical data from 2002 and recent LANDSAT images from 2022. Future iterations of the heat transfer model could incorporate relative humidity data and LANDSAT image data to improve accuracy of evaporative cooling and incoming solar radiation estimates. Modeling the relationship between ground temperature and weather patterns within the densely populated island of Manhattan contributes to our understanding of the urban heat island effect and its impact on NYC residents.**

I. Introduction

New York City is the most highly populated city in the United States. Dense cities, such as NYC, are known to experience a phenomenon called the Urban Heat Island Effect. This phenomenon occurs when the air temperature in urban areas is significantly higher than that in the surrounding rural areas. Increased heat makes life in cities very challenging in the summers. Not only is heat a daily inconvenience, but it can also cause medical issues, such as heat stress. In extreme cases, the urban heat island effect can even become fatal. Every summer in New York City, 370 people on average die of heat-related causes. This amounts to 2% of all deaths occurring in this time period [1]. Some factors contributing to the heat island effect are known. These include increased absorption of solar radiation, air pollution, anthropogenic heat, heat storage, impermeable surfaces, and reduced wind speed [2]; however, the exact heat transfer mechanisms causing temperature variation within urban landscapes are not as well understood. Therefore, modeling temperature and weather variations within cities presents an important opportunity to improve understanding of how urban heat islands function. Better understanding of urban heat islands can guide critical urban planning decisions to protect the lives and homes of NYC residents faced with an ever-warming climate.

The authors are with the Department of Mechanical Engineering, Columbia University, New York, NY.

Compared to the dominantly suburban and rural landscapes of the United States, NYC is a considerable outlier. Yet, within this dense concrete landscape, NYC also has a huge park - Central Park. Due to this stark contrast between built concrete environments and the greenery of Central Park, Manhattan experiences noticeable variations in temperature and weather patterns in different parts of the city. We are interested in understanding the differences in heat transfer and resulting temperatures in vegetated ground compared to concrete within NYC. Our goal is to build a model that accurately predicts ground temperature in various NYC locations and reproduces expected trends, such as the observation that ground temperature in vegetated areas is lower than concrete ground.

In order to address the question of predicting ground temperature in different places in NYC, we chose several Manhattan locations with predominantly concrete environments and compared the maximum air temperatures, wind speeds, and ground temperatures at different stations and at Central Park. Air temperature and wind speed data were taken from various Weather Underground weather stations in Manhattan. The Weather Underground stations in New York are presented in Figure 1.

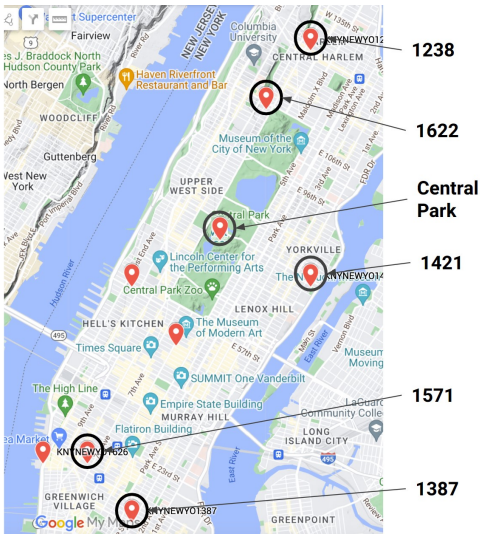

Fig. 1. Weather Underground (WU) stations in NYC.

To compare heat transfer from concrete and vegetation, we used two different models for the ground – one for each material. Both models include incoming solar radiation, convection to the air, and radiation from the ground to the sky. The vegetated model also includes evaporative cooling, while the concrete model does not. The other difference between

vegetation and concrete is the emissivity. The emissivity of vegetation is higher than that of concrete due to its higher water content. A higher emissivity radiates more heat from the ground to the sky, so the ground temperature will be cooler. For each heat transfer model, we assumed steady state conditions and found the energy balance for a slab of ground:

$$\begin{aligned} \Sigma E &= q_{in} - q_{out} = 0 \\ \rightarrow q_{in} &= q_{out} \end{aligned} \tag{1}$$

Let's define q_{in} using the incoming solar radiation q_{solar} and q_{out} as the convection from the ground to the air, defined as q_{conv}. For vegetated ground, the convection from the ground to the air occurs in parallel with q_{evap}, the evaporation from the ground to the air, and $q_{rad-to-sky}$, the radiation from the ground to the sky [3].

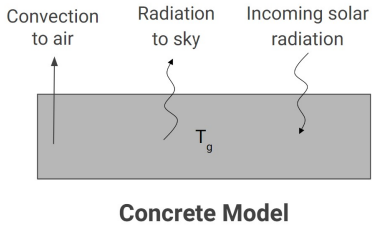

Fig. 2. Heat transfer model of concrete.

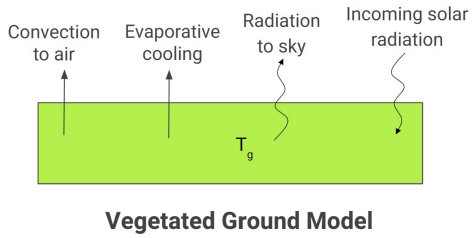

Fig. 3. Heat transfer model of vegetated ground.

These observations give us the equations for heat transfer in the case of zero evaporation (concrete) and non-zero evaporation (vegetated ground):

$$q_{solar} = q_{rad-to-sky} + q_{conv} + q_{evap} \tag{2}$$

Inputting air temperature and wind speed data from Weather Underground, we were able to predict the ground temperature and compare it to measured values.

II. Methods

To create a model of heat transfer on the ground, we derived a linear approximation for heat transfer of vegetated and non-vegetated ground through several modes: convection to the air, evaporation from the ground, incoming solar radiation, and radiation from the ground to the sky. We used this model to predict ground temperatures at various stations in New York City based on measured temperature, wind speed, average rainfall, time of year, and ground composition (vegetated or concrete).

A. Convection: Flow over a flat plate

We assume that the weather station is measuring the air temperature. We assume that all measurements (temperature, wind speed, humidity, etc) from a weather station are taken in the same location (not at different heights off the ground). We assume that this location is at least 5 feet above the ground, per Weather Underground's recommendations for siting the temperature measurement for a personal weather station [4].

To approximate the the Reynold's number (Re), we use the following equation,

$$Re = \frac{\rho u L}{\mu}, \tag{3}$$

where ρ = fluid density, u = velocity of the free stream, L = characteristic length, and μ = fluid viscosity.

We start by defining the characteristic length L, using

$$L = \text{length of 1 NYC block} = 80\ m.$$

Next, we define the properties of the air. We assume that the air is at atmospheric pressure and a standard temperature of 16 deg C, which corresponds to $289K$. The dynamic viscosity of the air with these conditions is $17.93\text{Pa s} \cdot 10^{-6}$ [5]. We assume that the dynamic viscosity of air does not change with temperature for simplicity.

The density of air, ρ, can be calculated from

$$\rho = \frac{p}{R_{air} T} \tag{4}$$

and

$$R_{air} = \frac{R}{M}, \tag{5}$$

where $R = 8.314J\ K^{-1}mol^{-1}$ is the ideal gas constant, and M is the molar mass of the air = .029 kg/mol [6].

Plugging in these numbers gives

$$R_{air} = \frac{8.314}{0.029} = 287JK^{-1}mol^{-1}. \tag{6}$$

Thus, we can find the density of air

$$\rho = \frac{101,325Pa}{287JK^{-1}mol^{-1}289K} = 1.22\frac{kg}{m^3}. \tag{7}$$

Using an example value of the wind speed, u = 5 m/s, we can calculate an example Reynold's number:

$$Re = \frac{\rho u L}{\mu} = \frac{1.22\frac{kg}{m^3} \cdot 5\frac{m}{s} \cdot 80m}{17.93Pa \cdot s \cdot 10^{-6}} \tag{8}$$

This gives $Re = 28,000,000 = 2.8 \cdot 10^7$.

The transition from laminar to turbulent flow in an external flow across a flat plate occurs in the range of Re = $5 \cdot 10^4$ to $5 \cdot 10^5$ [7].

In order to validate our assumption that all fluid flow was in the turbulent regime, wind speeds (Figure 4) and Reynold's numbers (Figure 5) were plotted at all weather stations within the date range of interest. The results confirmed that even at low wind speeds, the Reynold's numbers were well within the turbulent regime, above Re = 10^7, which agrees with our turbulent assumption.

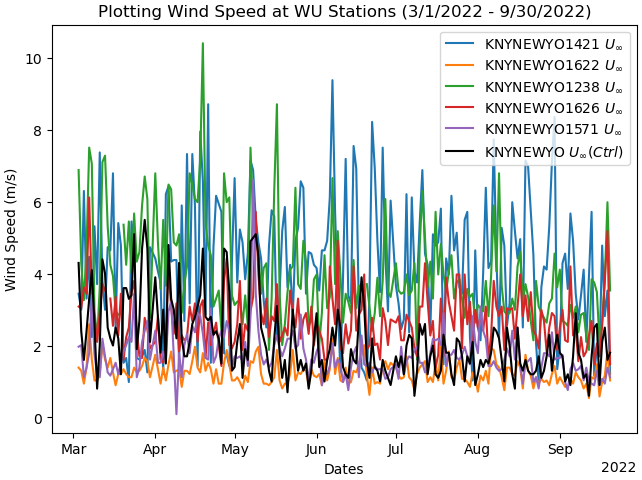

Fig. 4. Wind speed data at WU Stations.

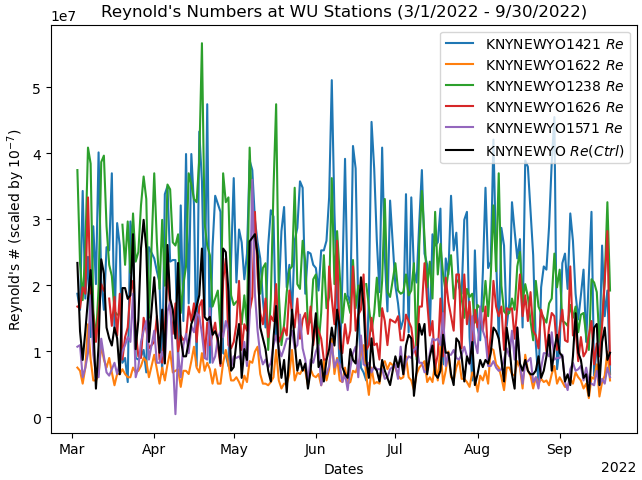

Fig. 5. Reynold's numbers calculated for WU Stations.

The convection from the hot ground to the air can be modeled as an external forced flow over a flat plate. The average heat transfer coefficient, $\bar{h}$, can be found from the following empirical correlation for turbulent flow over a flat plate [8]:

$$\bar{Nu} = \frac{\bar{h}L}{k} = 0.037 Re_L^{4/5} Pr^{1/3} \tag{9}$$

Solving for $\bar{h}$ gives

$$\bar{h} = \frac{0.037 \cdot k \cdot Re_L^{4/5} \cdot Pr^{1/3}}{L} \tag{10}$$

The Prandtl number for air, Pr_{air}, at 1 atm of pressure and temperatures between 0 and 50 degrees C, is 0.71 [9]. The thermal conductivity of air at 16 C and 1 atm is $0.02557 Wm^{-1}K^{-1}$ [10].

Assume that the thermal conductivity of air does not vary much with temperature. Using Pr = 0.71, Re depends on the wind speed on that day, L = 80 m, k = $0.02557 Wm^{-1}K^{-1}$,

$$\bar{h} = \frac{0.037 \cdot 0.02557 Wm^{-1}K^{-1} \cdot Re_L^{4/5} \cdot 0.71^{1/3}}{80m} \tag{11}$$

Continuing our previous example with u = 5 m/s and $Re = 2.8 \cdot 10^7$, an example h value is 9.6 $Wm^{-2}K^{-1}$.

The convective heat transfer coefficient for each day, based on that day's wind speed, can be used to find the convective heat transfer, q_{conv}:

$$q_{conv} = h(T_g - T_a) \tag{12}$$

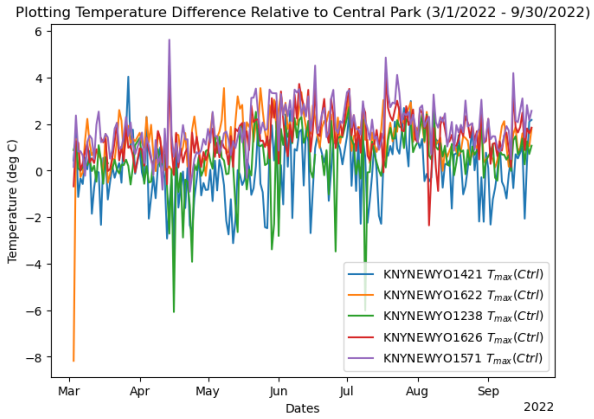

Fig. 6. Difference between air temperatures measured at WU stations and Central Park.

The temperature of the air, T_a, is the maximum daily temperature, as taken from Weather Underground stations. The maximum daily temperature was used to see the maximum urban heat island effect each day rather than changes over the course of the day. Figure 6 shows the difference between the maximum daily air temperature at each station compared to the maximum daily air temperature at Central Park. Most stations are consistently warmer than Central Park, indicated by a positive temperature difference in Figure 6. This trend is especially prevalent in the summer months. Stations 1421 and 1238, which have higher wind speeds, have lower air temperatures than the other stations during the measured time interval. These stations correspond to the blue and green lines in Figure 4. This observations suggest that lower air temperatures are associated with higher rates of convective heat transfer.

B. Heat lost from ground to air through evaporation

The amount of heat lost by the ground and gained by the air due to evaporation is equal to the latent heat:

$$q_{evap} = h_L \cdot m \tag{13}$$

where h_L is the latent heat of evaporation for water, assumed to be 2256 kJ/kg of water, and m is the mass of water evaporated. [11]

$$\begin{aligned} q_{evap} &= h_L \cdot \text{mass} \\ &= h_L \cdot \rho \cdot \text{volume} \\ &= h_L \cdot \rho \cdot \text{length} \cdot \text{width} \cdot \text{depth} \end{aligned} \tag{14}$$

Water is assumed to have a density of 1000 kg/m^3. The height of water evaporated per second is found from `https://docs.google.com/spreadsheets/d/`

1YsoljxFvVrdrBg8EVf7xXc5aplNNJnqOb9dwC9rTni0/edit#gid=0.

The heat lost to evaporation, $q_{evap} = h \cdot \rho \cdot l \cdot w \cdot d$, where d is the depth of the water.

$$q_{evap} = 2256\frac{kJ}{kg} \cdot 10^3 \frac{J}{1\ kJ} \cdot 10^3 \frac{kg}{m^3} \cdot 1\ m \cdot 1\ m \cdot d \quad (15)$$

Depth of water evaporated was computed from taking monthly total precipitation in New York City. LaGuardia Airport's weather data [12] was used for this since few stations had historical precipitation data. Precipitation is assumed to be the same throughout the city. The measured precipitation rate in inches per month was converted to m/s. We assumed that 60% of the rainfall evaporates and the remaining 40% is absorbed or runs off [13], so we multiplied the precipitation rate in m/s by 0.6 to find the evaporation rate in m/s. This number was plugged in for d in equation 15 to find the rate of heat evaporation for each month.

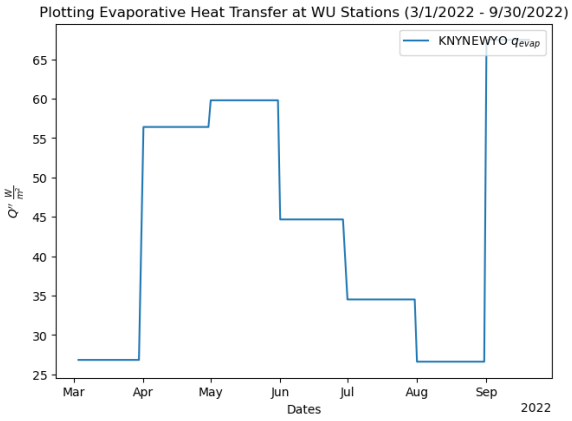

Fig. 7. Evaporative heat transfer calculated by month using collected rainfall data.

C. Solar Radiation

The maximum daily solar radiation is a function of the solar constant, q_s, multiplied by a constant α_s which accounts for the amount of solar radiation reflected and absorbed by the atmosphere. The value q_s is equivalent to the total solar radiation 1362 Wm^{-2} divided by 4, which is 340.5 Wm^{-2} [14]. The value of α_s varies depending on the amount of cloud cover in the sky. Typical values for α_s range from 0.7 on clear, sunny days to 0.5 on cloudy days [14]. The average value for q_{solar} is

$$q_{solar} = q_s \cdot \alpha_s = 340.5 \cdot 0.6 = 204.3\ Wm^{-2}$$

We will conduct a sensitivity study to bound our error due to varying cloud cover. Specifically, we will put upper and lower bounds on the value of q_{solar} by using $\alpha_s = 0.7$ and $\alpha_s = 0.5$, respectively. For the purpose of deriving the heat transfer model equations, we use the average maximum daily solar radiation of approximately 200 Wm^{-2}[15]. This value depends on the day of the year and varies with the sine of the angle of the sun's elevation at solar noon, such that

$$q_s \cdot \alpha_s = 200\ W\ m^{-2} \cdot sin(\beta_N), \quad (16)$$

where

$$\beta_N = 90 - L + \delta \quad (17)$$

and β_N is the angle of the sun's elevation at solar noon, L is the latitude (40.7 degrees for NYC), and δ is the declination [16].

The declination, δ, is calculated as a function of the day of the year, n [16]:

$$\delta = 23.45\ sin(\frac{360}{365}(n - 81)) \quad (18)$$

So, combining these,

$$\alpha_s q_s = 200 \cdot sin(90 - 40.7 + 23.45 \cdot sin(\frac{360}{365}(n - 81))) \quad (19)$$

Although variations in cloud cover also impact incoming solar radiation, we neglected this from our model for simplicity. Relative humidity, which is correlated with cloud cover, does not appear to vary much from station to station (see Figure 8), so we assume that cloud cover is also consistent from station to station.

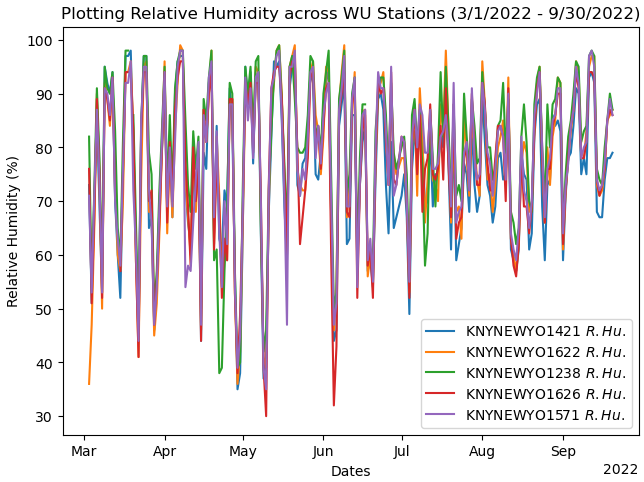

Fig. 8. Relative humidity measured at NYC weather stations.

This graph shows that our assumption is valid, since there is not much of a difference between humidity at the different stations.

D. Radiation from Ground to Sky

Heat lost from the ground to the sky due to radiation is computed using the linearization of the radiative heat transfer equation,

$$q_{rad} = \sigma\epsilon(T^4 - T_0^4) = 4\sigma\epsilon T_0^3(T - T_0) \quad (20)$$

where σ is the Stefan-Boltzmann Constant equaling $5.670 \cdot 10^{-8}\ W\ m^{-2}K^{-4}$, ϵ is the emissivity and equals 0.85 for concrete [17] and 0.97 for vegetation [18], T is the ground temperature, and T_0 is the sky temperature, which is assumed to be 280 K [15].

E. Full Model

Substituting the equations for q_{conv}, q_{evap}, q_s, and $q_{rad-to-sky}$ into (2) gives

$$\alpha_s q_s = 4\sigma\epsilon T_{sky}^3(T_g - T_{sky}) + h(T_g - T_a) + q_{evap}. \quad (21)$$

Using T_a as an input and solving for T_g, we can solve for the ground temperature

$$T_g = \frac{\alpha_s q_s + hT_a + 4\sigma\epsilon T_{sky}^4 - q_{evap}}{h + 4\sigma\epsilon T_{sky}^3}. \quad (22)$$

F. Data Analysis

All data analysis was performed in Python using the Pandas library for data processing and Matplotlib for data visualization.

The data for Central Park was accessed via the National Oceanic and Atmospheric Administration (NOAA) datasets [19], and the data for the remaining weather stations was scraped from Weather Underground (WU) websites and compiled into csv files [12]. Step-by-step descriptions of data filtering, unit conversion, calculations, visualizations, and comparison to historical data are included in the following Jupyter notebook `https://github.com/soph-loaf/aht_project/blob/ca179ecc664fe111803e6364856e906f2c722b0d/Temperature_Modeling_Results_SAL.ipynb`, which is included within the "aht_project" repository hosted on GitHub. The datasets themselves and functions used to implement the heat transfer model are accessible within the same repository.

For this analysis, we decided to use only the maximum temperature value for each day for each weather station to build our heat transfer model. Although this assumption reduced the amount of data we could use, it allowed us to greatly simplify the heat transfer model. We expect these temperatures to correspond to the peak solar radiation. Thus, we could easily model the solar radiation absorbed by the ground, q_{solar}, and radiation from the ground to the sky, $q_{rad-to-sky}$, as a function of the time of year and latitutde and longtitude of New York City.

We considered several methods to increase the number of data points in our model, such as comparing minimum, mean, and maximum temperatures per day, or grouping the max temperature by each hour; however, taking data from other times of data, especially night time, would require adding transient conditions to the heat transfer model to account for the heat dissipation from the ground to the sky at night. We decided that for the goal of analyzing heat transfer in dense, populated environments subject to the urban heat-island effect, a steady-state model using max daily temperatures would be much more useful than attempting to account for transient night-time effects.

III. Results and Discussion

The following results include predicted ground temperatures for weather stations and Central Park.

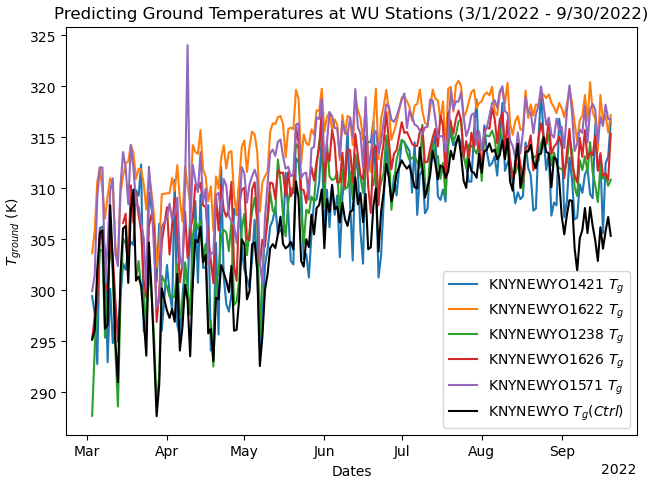

Fig. 9. Predicted ground temperature assuming constant solar radiation ($\alpha_s q_s = 200 Wm^{-2}$).

Figure 9 shows that while there is variation in predicted ground temperature among stations, the predicted ground temperature at Central Park, the black line, is consistently lower than that at other stations. Additionally, the ground temperature at Central Park in September is exceptionally low. This makes sense because September 2022 has much more precipitation than the other months here, so it would have more evaporative heat transfer, resulting in a lower ground temperature. The concrete surfaces at other stations did not experience evaporative cooling under our model, so it makes sense that their ground temperatures did not decrease as a result of increased rain.

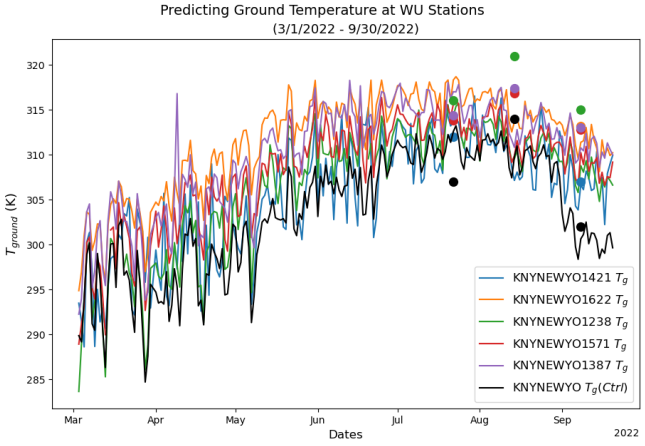

Fig. 10. Predicted ground temperature accounting for variable solar radiation and compared to 2002 ground temperatures.

Figure 10 builds on Figure 9 by varying the solar radiation with the time of year using equation 19. Figure 10 has more of a peak in July than Figure 9, which is roughly constant for the whole summer. This is now the full model. We observe that the green and blue lines on this graph correspond to stations where the wind speeds are greater, as seen in Figure 4. The ground temperatures at these stations are also predicted by our model to be lower as a result.

The predicted ground temperatures were compared to historical ground temperature data on three dates: July 22nd, August 14th, and September 8th, 2002. These are represented

with dots on the graph. The colors of the dots match the colors of the lines. Although the dots don't match up with the lines exactly, they are in the same range and follow the same trends. We did not expect them to match up exactly because the data is from a different year, 2002, with different weather conditions that would impact the ground temperature; however, the trends in the measured data do agree with our model predictions. The measured ground temperatures are within the approximate 305-315 K range of the modelled stations for that time of year, and the September ground temperatures are lower than those in July and August. Additionally, the measured ground temperature in Central Park is much lower than the measured ground temperatures at other stations, as we would expect, and as our model predicts as well.

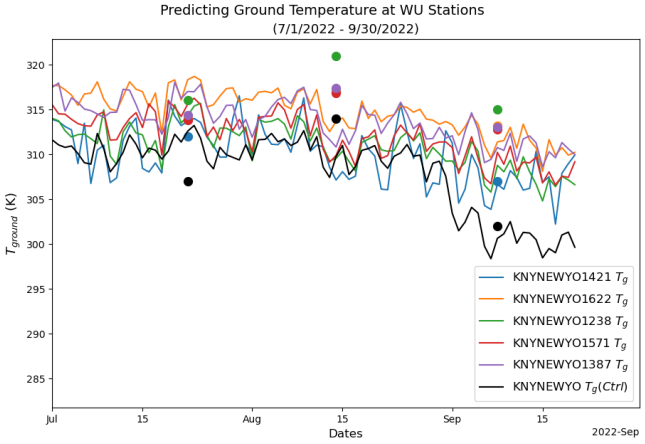

Fig. 11. Predicted ground temperature compared to historical data for ground temperatures in 2002.

Figure 11 is a zoomed-in version of Figure 10, concentrated just on the months July-September. The differences between the dots and the lines can be seen more clearly.

We also compared our model's predictions to the measured ground surface temperatures on the following three dates: July 22, August 14, and September 8. The ground temperature values for each location are given in Figure 12.

		Measured Ground Temperature (K) *Historical Data, 2002*			Predicted Ground Temperature (K) *Recent Weather Data, 2022*		
Station	**Location**	**7/22/2002**	**8/14/2002**	**9/8/2002**	**7/22/2022**	**8/14/2022**	**9/8/2022**
1421	near East River	312	317	307	313.7	307.1	306.7
1622	Central Park North	314	317	313	318.3	313.7	311.4
1238	Central Harlem	316	321	315	314.3	309.5	308.8
1571	Lower west side	314	317	313	315.6	309.9	310.2
1387	Lower east side	314	317	313	317.0	310.8	310.8
Central Park	Central Park	307	314	302	312.6	309.8	300.6

Fig. 12. Measured vs. Predicted Ground Temperatures

Percent error is given in Figure 13. The percent error was less than 30% for all stations and dates and was less than 1% in some cases. The average percent error is 12%.

Overall, comparing our predicted ground temperatures to historical data suggests that our model is able to reasonably approximate trends in weather patterns over time and at parks compared to built environments in NYC. Still, our

Station #	**7/22 % Error**	**8/14 % Error**	**9/8 % Error**
1387	0.4%	30%	17%
1421	14%	9%	12%
1622	1%	22%	10%
1238	0.1%	30%	13%
1571	7%	17%	4.5%
Central Park	15%	11%	5%

Fig. 13. Percent Error

model has several shortcomings that could be improved with future work. In particular, the models for evaporative heat transfer and incoming solar radiation could be improved by accounting for the effects of humidity and cloud cover. By omitting humidity from our current model, we likely overestimate the heat loss due to evaporative cooling on extremely humid days because the accumulated water on vegetated ground cannot evaporate as easily when there is high relative humidity in the air. Thus, adding humidity as an input variable to our model could improve the accuracy of our estimate for the evaporative heat transfer in vegetated areas.

Creating a model to accurately capture the effects of incoming solar radiation is quite challenging, due to the many variables involved. For example, we know that cloud cover affects the value of α_s, but there is no simple way to measure cloud cover and derive a linear relationship to predict how much a certain amount of cloud cover will diminish incoming solar radiation. In addition, there are particular barriers involved in obtaining and using cloud cover data. Weather Underground includes only subjective measurements of cloud cover (e.g. "Mostly Cloudy"), which could vary depending on the observer's judgment. Cloud cover also varies throughout the day, and more cloud cover in the morning could decrease the maximum air temperature later in the day. Our existing model assumed steady state during max temperature measurements and neglected daily temporal variations. Instead, we accounted for variations in incoming solar radiation by performing a sensitivity study to bound the expected values for T_g according to the uncertainty of α_s. Figures 14 and 15 show the variation in predicted T_g for central park and weather station 01622, located near Central Park North. Figure 16 shows predicted ground temperatures for both stations, with the upper and lower bounds ($\alpha_s = 0.7$ and $\alpha_s = 0.5$ respectively) represented by smoothed lines in order to bound the data. Bounded temperature data using the uncertainty of α_s is an effective way to validate our preliminary model, but incorporating the amount of cloud cover at each hour, along with the solar radiation at each hour, could make the model more complete.

Relative humidity, which Weather Underground does report, could be used as a proxy for cloud cover, since humidity and cloud cover are positively correlated, but that approach has limitations as well. When clouds are high in the atmosphere, cloud cover and humidity are not as related as when clouds are close to the ground [20]. Without knowing the cloud height, there would be uncertainty in

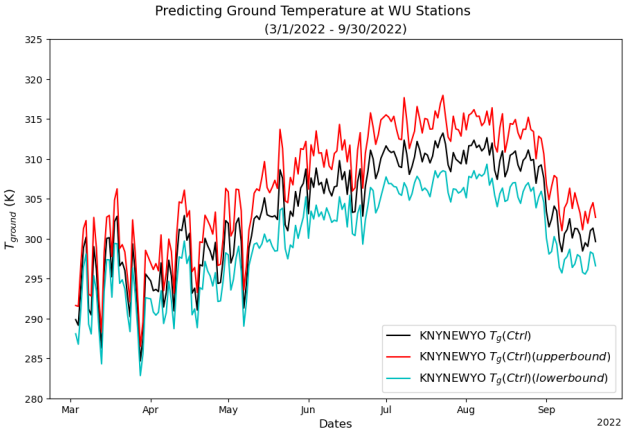

Fig. 14. Sensitivity study on Central Park ($\alpha_s = 0.5, 0.6, 0.7$)

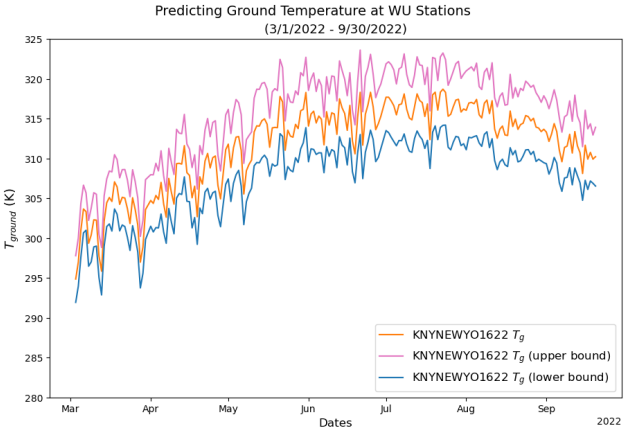

Fig. 15. Sensitivity study on Station 1622 ($\alpha_s = 0.5, 0.6, 0.7$)

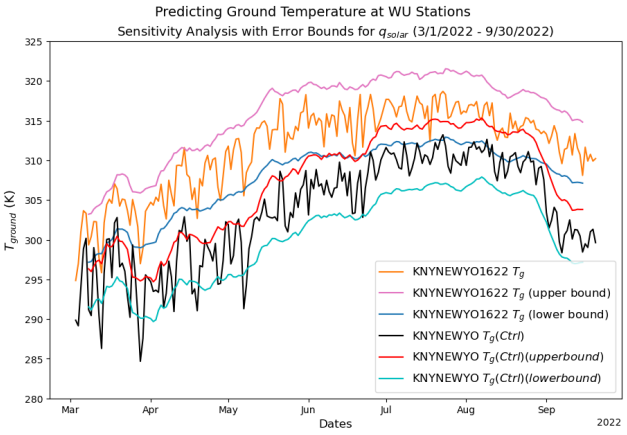

Fig. 16. Sensitivity study on Station 1622 compared to Central Park ($\alpha_s = 0.5, 0.6, 0.7$)

the cloud cover computed from the relative humidity. For these reasons, for future research, we recommend using cloud cover data directly from satellite imagery like LANDSAT [21]. By adding humidity data from Weather Undergroud and cloud cover data from LANDSAT satellite datasets, we could improve our model's estimation of evaporative heat transfer and incoming solar radiation.

In addition to the historical measured ground temperature data from 2002, we wanted to compare predicted ground

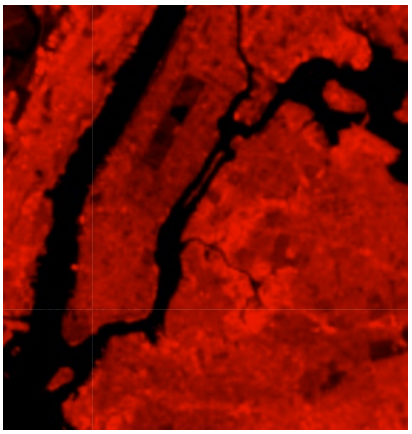

Fig. 17. Ground temperature data from LANDSAT images.

temperatures with measured ground temperature data from the same date ranges in 2022. Figure 17 shows a map of ground temperature data extracted from LANDSAT 9 data captured on July 22, 2022 [21]. The map shows hotter areas in red and cooler areas in black. We observe similar trends in the July 22, 2022 temperature distribution in NYC to the historical data from 2002, with Central Park being cooler than other parts of the city. The similarity in spatial temperature trends between this July 22, 2022 LANDSAT image and the historical July 22, 2002 image support using 2002 image data to validate our model. In the future, we hope to obtain quantitative ground temperature data from LANDSAT images during the March to September, 2022 months and recalculate the average percent error of our predicted ground temperatures.

IV. Conclusion

Our heat transfer model successfully represented the trends in ground temperature data based on historical comparisons, finding that ground temperature is in the 290-320 K range, peaks in the summer as solar radiation increases, and decreases with increased wind speed, evaporation, and emissivity of the ground. The percent error between our estimated ground temperatures and historical ground temperatures on three dates across weather stations in NYC was 10-20% on average.

Future research in the area of modeling temperature variations within urban environments could incorporate surface temperature and cloud cover data from satellites like LANDSAT, as well as relative humidity data from conventional weather stations, for improved accuracy of incoming solar radiation and evaporative heat transfer calculations.

References

[1] "2022 new york city heat-related mortality report." https://nyccas.cityofnewyork.us/nyccas2022/report/1.

[2] L. Kleerekoper, M. van Esch, and T. B. Salcedo, "How to make a city climate-proof, addressing the urban heat island effect," *Resources, Conservation and Recycling*, vol. 64, 2012.

[3] R. K. Singh and R. V. Sharma, "Numerical analysis for ground temperature variation," *Geothermal Energy*, vol. 5, 2017.

[4] "Installing your personal weather station." https://www.wunderground.com/pws/installation-guide.

[5] "Air - dynamic and kinematic viscosity." https://www.engineeringtoolbox.com/air-absolute-kinematic-viscosity-d_601.html.
[6] "Air - molecular weight and composition." https://www.engineeringtoolbox.com/molecular-mass-air-d_679.html.
[7] A. Mills, *Heat and Mass Transfer*. Routledge, 1. ed., 1995.
[8] T. L. Bergman, A. S. Lavine, F. P. Incropera, and D. P. Dewitt, *Fundamentals of Heat and Mass Transfer*. John Wiley Sons, Inc., 7. ed., 2011.
[9] "Air - prandtl number." https://www.engineeringtoolbox.com/air-prandtl-number-viscosity-heat-capacity-thermal-conductivity-d_2009.html.
[10] "Air - thermal conductivity vs. temperature and pressure." https://www.engineeringtoolbox.com/air-properties-viscosity-conductivity-heat-capacity-d_1509.html.
[11] "Liquids - latent heat of evaporation." https://www.engineeringtoolbox.com/fluids-evaporation-latent-heat-d_147.html.
[12] "Weather underground weather history for knynewyo1421." https://www.wunderground.com/dashboard/pws/KNYNEWYO1421/table/2022-03-1/2022-03-1/daily. This is an example link for one day for one weather station.
[13] D. Or, P. Lehmann, E. Shahraeeni, and N. Shokri, "Advances in soil evaporation physics—a review," *Vadose Zone Journals*, vol. 12, 2013.
[14] G. Kopp and J. L. Lean, "A new, lower value of total solar irradiance: Evidence and climate significance," 2011.
[15] A. Narayanaswamy. Advanced Heat Transfer Class Notes, 2023.
[16] V. Modi. Energy Sources and Conversion Class Notes, 2020.
[17] "Emissivity coefficients common products." https://www.engineeringtoolbox.com/emissivity-coefficients-d_447.html.
[18] J. Nichol, "An emissivity modulation method for spatial enhancement of thermal satellite images in urban heat island analysis," *Photogrammetric Engineering and Remote Sensing*, vol. 75, 2009.
[19] Menne, M.J., I. Durre, B. Korzeniewski, S. McNeill, K. Thomas, X. Yin, S. Anthony, R. Ray, R. Vose, B.E.Gleason, , and T. Houston, "Global historical climatology network - daily (ghcn-daily), version 3.30," *NOAA National Climatic Data Center*, 2012. Accessed: 2023-04-30.
[20] C. J. Walcek, "Cloud cover and its relationship to relative humidity during a springtime midlatitude cyclone," *Monthly Weather Review*, vol. 122, 1994.
[21] "Earth engine data catalog: Usgs landsat 9 level 2, collection 2, tier 1." https://developers.google.com/earth-engine/datasets/catalog/LANDSAT_LC09_C02_T1_L2.

V. Appendix

Contributions:

We both contributed equally to this project. I would assign 50% contribution to both myself and Sally. - SL

I second that. I would also assign 50% contribution to each of us. - SG

Github repository for code:

`https://github.com/soph-loaf/aht_project`

Percent error formula:

$$\% \text{ error} = \frac{T_{predicted} - T_{observed}}{T_{predicted}} \cdot 100$$

Historical ground temperature images:

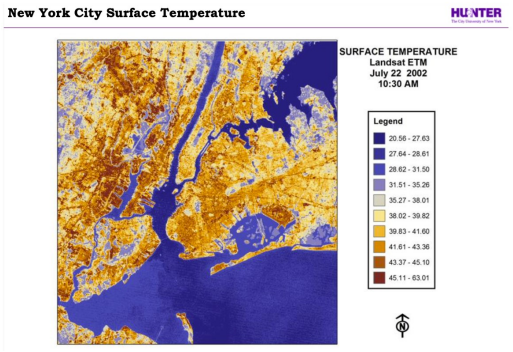

Fig. 18. NYC ground temperature historical data for July 22, 2002.

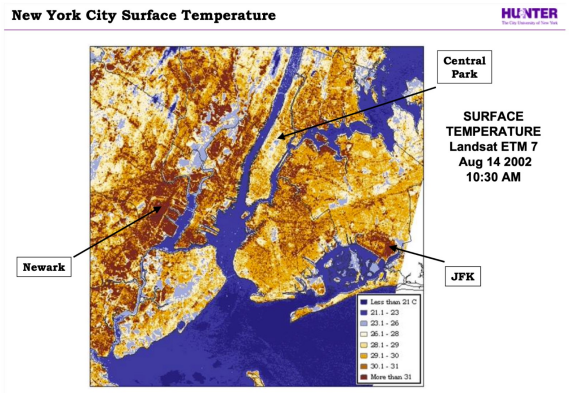

Fig. 19. NYC ground temperature historical data for August 14, 2002.

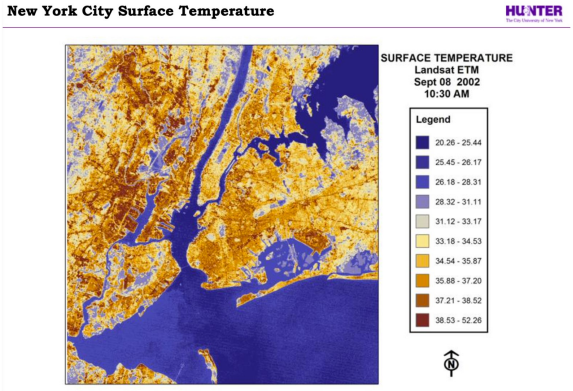

Fig. 20. NYC ground temperature historical data for September 8, 2002.